BIOCELL
2020 44(4): 655-669

Tech Science Press

20(R)-ginsenoside Rg3, a product of high-efficiency thermal deglycosylation of ginsenoside Rd, exerts protective effects against scrotal heat-induced spermatogenic damage in mice

Wei LIU[1,#]; Zi WANG[1,2,#]; Jing LENG[1]; Heng WEI[1]; Shen REN[1,2]; Xiaojie GONG[3]; Chen CHEN[4]; Yingping WANG[1,2]; Rui ZHANG[1,2,*]; Wei LI[1,2,*]

[1] College of Chinese Medicinal Materials, Jilin Agricultural University, Changchun, 130118, China
[2] National & Local Joint Engineering Research Center for Ginseng Breeding and Development, Changchun, 130118, China
[3] Key Laboratory of Biotechnology and Bioresources Utilization, College of Life Science, Dalian Minzu University, Dalian, 116600, China
[4] School of Biomedical Sciences, University of Queensland, Brisbane, 4072, Australia

Key words: 20(R)-ginsenoside Rg3, Heat stress, Spermatogenic damage, Oxidative stress, MAPK

Abstract: Heat stress (HS) reaction can lead to serious physiological dysfunction associated with cardiovascular and various organ diseases. Ginsenoside Rg3 (G-Rg3) is a representative component of ginseng rare saponin and can protect against multiple organs, also used as functional food to adjust the balance of the human body, but the therapeutic effect and molecular mechanism of G-Rg3 on male diseases under HS are underexplored. The aim of the present study, G-Rg3 was prepared through the efficient conversion of ginsenoside Rd and investigate the contribution of G-Rg3 to testicular injury induced exposure to HS. All mice were divided into four groups as follows: normal group, HS group, and HS+G-Rg3 (5 and 10 mg/kg) groups. G-Rg3 was administered orally for 14 days, then exposed to a single scrotal heat treatment (43°C, 18min) on the 7th day. After HS treatment, the morphology of testis and epididymis changes, and caused a significant loss of multinucleated giant cells, desquamation of germ cells in destructive seminiferous tubules, and degenerative Leydig cells, further destroying the production of sperm. After administration G-Rg3 (5 and 10 mg/kg/day) for 2 weeks, the spermatogenic-related indexes of testosterone levels and superoxide dismutase (SOD) activity, glutathione (GSH) content significantly ($p < 0.01$) increase compared with the HS group. Moreover, G-Rg3 treatment effectively ameliorated the production of malondialdehyde (MDA) ($p < 0.05$ or $p < 0.01$). Importantly, G-Rg3 exhibited the protective potential against HS-induced injury not only suppressing the protein levels of heme oxygenase-1 (HO-1), hypoxia-inducible factor-1α (HIF-1α), and heat shock protein 70 (HSP70) but also modulating the Bcl-2 family ($p < 0.01$ or $p < 0.001$) and activation of mitogen-activated protein kinase (MAPK) signaling pathways ($p < 0.01$). For most of the parameters tested, the HS+G-Rg3 (10 mg/kg) group exhibited potent effects compared with those exhibited by the low dose (5 mg/kg) group. In conclusion, the present study demonstrated that G-Rg3 exerted protective effects against HS-induced testicular dysfunction via inhibiting the MAPK-mediated oxidative stress and apoptosis in mice.

Abbreviations

HS:	Heat stress
PPD:	protopanaxadiol
MDA:	Malondialdehyde
SOD:	Superoxide dismutase
GSH:	Glutathione
HIF-1α:	Hypoxia inducible factor-1α
HSP70:	Heat shock protein 70
HO-1:	Heme oxygenase-1
MAPK:	Mitogen-activated protein kinase
JNK:	c-Jun N-terminal kinase
ERK:	Extracellular signal-regulated kinase

*Address correspondence to: Rui Zhang, zr99101@163.com; Wei Li, liwei7727@126.com
#These authors contributed equally to this work
Received: 29 July 2020; Accepted: 03 September 2020

Introduction

Climate change is an important hazard to our environment and physical health, particularly the male reproductive

Doi: 10.32604/biocell.2020.013202

system (Agarwal *et al.*, 2015). Increasing heat stress (HS) reactions are emerging and becoming more prevalent because of modern lifestyle, including mental stress, smoking, high temperature, and air pollution adverse factors (De Blois *et al.*, 2015; Hughes and Acerini, 2008). Importantly, abundant evidence suggested that male reproductive dysfunction is closely related to environmental changes, affecting testicular quality and spermatogenesis significantly (Durairajanayagam *et al.*, 2015). This might be due to high temperatures increase the testicular metabolism lack of adequate blood supply and result in local hypoxia damaging the testicular tissue (Bromfield *et al.*, 2017; Lin *et al.*, 2016), which is corroborated by studies in a number of animal models (Shen *et al.*, 2019; Sui *et al.*, 2019). Therefore, the correction or prevention of heat-induced sterility is a problem of major concern.

Early experimental evidence by Phuge, Hu, and Cai, indicated that scrotal temperature is essential to maintaining an optimal environment in testicular function (Cai *et al.*, 2011; Hu *et al.*, 2019; Phuge, 2017). Recent studies have shown that scrotal temperatures above the normal range caused oxidative stress and germ cell death in testes, leading to male infertility (Han *et al.*, 2019; Zhang *et al.*, 2012). Moreover, continuing HS also lead to severe damages on the testis, such as hypoxia in testes and endogenous or exogenous toxins (including peroxide anions and hydrogen peroxide), and related to the DNA damage and repair (Paul *et al.*, 2008), and the production of hypoxia-inducible factor-1 (HIF-1) in the male germline.

HS reaction due to elevated temperatures involved in the activation of the transcription factor, such as HIF-1 (Baird *et al.*, 2006), also including the production of free radicals and reactive oxygen species (ROS) (Costa *et al.*, 2018). Spermatozoa are extremely sensitive to ROS-induced damage (Aitken and Clarkson, 1987). Meantime, overproduction of ROS can induce spermatogenesis-related negative changes, such as sperm capacitation and acrosome reaction (Castillo *et al.*, 2019; Stival *et al.*, 2016). As spermatogenesis is susceptible to oxidative stress, and peroxidative injury is considered to be one of the important reasons for impaired testicular function (Houston *et al.*, 2018; Li *et al.*, 2014). Oxidative stress occurs also related to the disturbance of the antioxidant defense systems, such as the changes of lipid peroxidation malondialdehyde (MDA), glutathione (GSH), and superoxide dismutase (SOD) (Kim *et al.*, 2013a). Meanwhile, heme oxygenase-1 (HO-1) and heat shock protein 70 (HSP70), play a potential target in heat stress-induced spermatogenic cell disorders (Stahli *et al.*, 2019). Among heat shock proteins (HSPs) are a group of stress-responsive proteins expressed widely in various organs, and also vitally important in inhibiting cellular apoptosis, keeping intracellular homeostasis of redox, and maintaining mitochondrial integrity (Kim *et al.*, 2015). More importantly, oxidative stress could result in cell cycle arrest and trigger apoptosis, the delicate balance between oxidative stress (Niu *et al.*, 2020) and the apoptotic pathway is critical during the process of spermatogenesis (Xu *et al.*, 2019). Increasing evidence demonstrates that Bax, Bcl-2, and caspase family are involved in the regulation of apoptosis of germ cells and Leydig cells (Fischer and Schulze-Osthoff, 2005; Kheradmand *et al.*, 2012). Despite such a severe negative impact of HS on spermatogenesis, research on the specific mechanism of heat-induced spermatogenic damage is not clarified.

Panax ginseng C. A. Meyer is a health-promoting traditional Chinese medicine with long medication history, its saponins (ginsenosides) were considered as the main active ingredient of *P. ginseng* (Jin *et al.*, 2015). Especially, G-Rg3 is a representative rare saponin and the most important active component of *P. ginseng* processed products (Red or Black ginseng) (Kim *et al.*, 2019; Zhang *et al.*, 2020). Importantly, ginsenosides Rb1, Rb2, Rc, and Rd with sugar moieties attached to the β-OH at C-3 and/or C-20, the sugar moieties at C-3 or C-20 were deglycosylated and dehydrated by heat processing, and they were gradually changed into 20(S/R)-Rg3, Rk1, Rg5 (Lee *et al.*, 2009) and 20(S/R)-Rh2 (Fig. 1). Modern pharmacology research showed G-Rg3 was effective for various diseases, such as anti-tumor, protects against multiple organ damage, promoting immune response, and numerous powerful pharmacological effects (Kim *et al.*, 2020; Park *et al.*, 2020). Further, *P. ginseng* has been traditionally used for therapeutic in boosting libido and treating infertility in men (Park *et al.*, 2016). In recent years, increasing studies on chemical, pharmacological and clinical aspects have proved that the pharmacological action of G-Rg3 provides broad prospects of the application (Fan, 2019; Phi *et al.*, 2019; Zhou *et al.*, 2018).

Previous studies have indicated that ginsenoside Rd through efficient thermal deglycosylation to conversion rare ginsenosides, and improved anticancer activity (Kim *et al.*, 2013b), but few studies have focused on the molecular mechanism through that rare ginsenosides treat a series of male diseases *in vivo*. Thus, in order to further develop natural products and better treat male diseases such as spermatogenic damage induced by HS. The present study aimed to use PPD-type ginsenoside Rd through high-temperature acid treatment to the purification of rare ginsenoside G-Rg3, and explored the effects and the available evidence on the role of G-Rg3 in HS-induced spermatogenic damage and provided its possible mechanism.

Materials and Methods

Sample preparation

G-Rg3 with a purity of 95.0% was the purification of rare ginsenoside from PPD-type ginsenoside Rd by formic acid treatment at 90°C. Specifically, take about 1.0 g of ginsenoside Rd powder, add 50 mL of 0.5% formic acid aqueous solution, and in a water bath at 90°C for 3 h by heat processing. The HPLC chromatogram of ginsenoside transformation products is illustrated in Fig. 2. The peak of ginsenoside Rd disappeared, and the peaks of ginsenoside 20 (S/R)-Rg3, Rk1, and Rg5, were newly detected in transformation products (Fig. 2B). The quantitative analysis of G-Rg3 was implemented on a Hypersil ODS2 column using high-performance liquid chromatography (Waters HPLC, Milford, MA, USA) at 203 nm. The detection method of HPLC, as previously described with a few adjustments (Xue *et al.*, 2017).

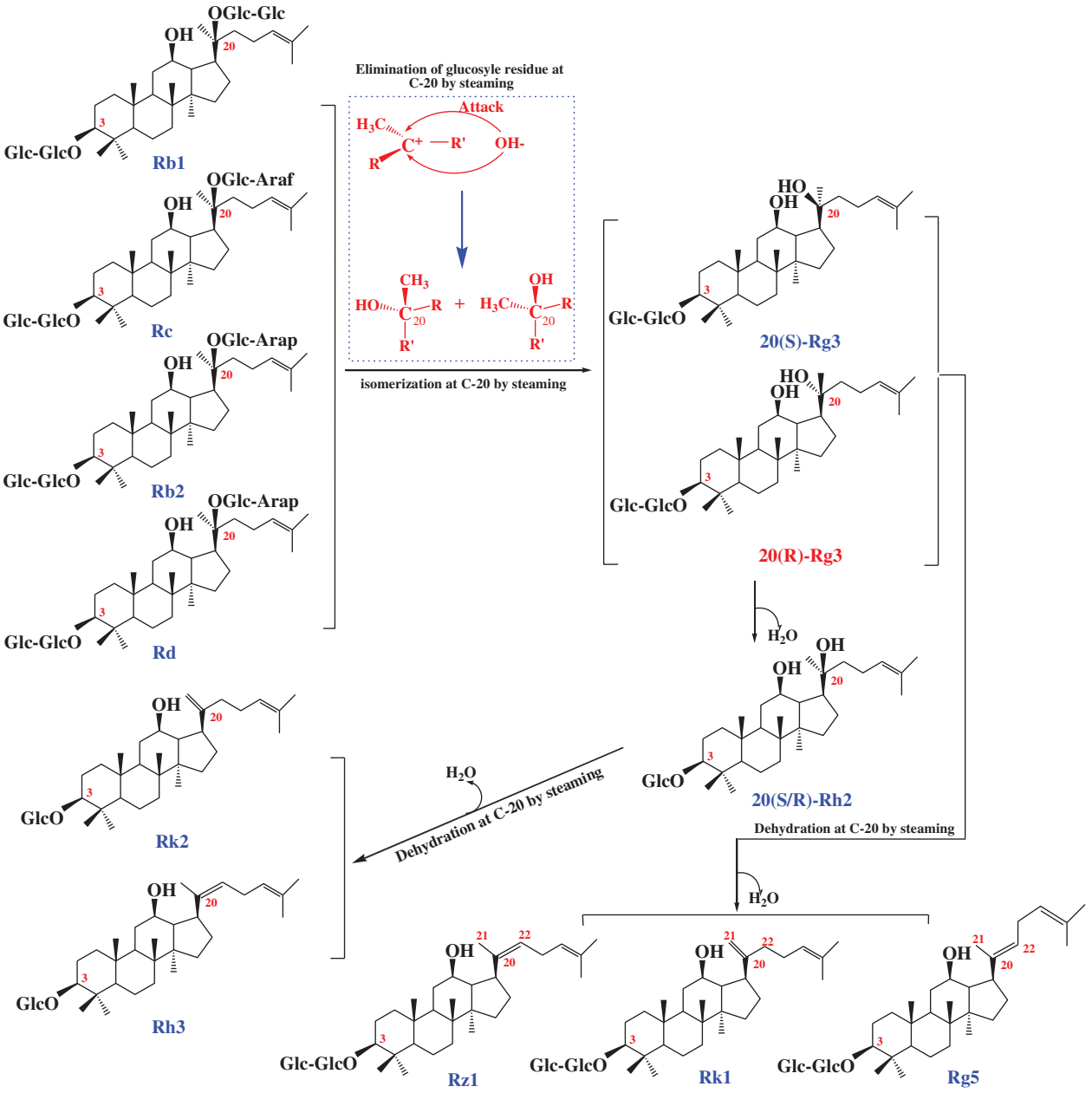

FIGURE 1. Diagram of the possible conversion process of protopanaxdiol-type 20(R)—ginsenoside Rg3.

Chemicals and Reagents

Ginsenoside Rd (CAS No. 52705-93-8, purity >95% by HPLC method) was obtained from PUSI Biotechnology Co. Ltd. (Chengdu, China). The hematoxylin-eosin (H&E), malondialdehyde (MDA, No. A003-1), glutathione (GSH, No. A006-1), and superoxide dismutase (SOD, No. A001-3) assay kits were purchased from Nanjing Jiancheng Bioengineering Research Institute (Nanjing, China). Testosterone (ELISA, No. KGE010) kit was bought from R&D Systems, Minneapolis (MN, USA). TUNEL apoptosis detection kits were bought from Promega (No. C1091, Madison, USA). Primary antibodies against HO-1, HIF-1α, HSP70, Bax, Bcl-2, Bcl-XL, JNK, p-JNK, ERK, p-ERK, p38, p-p38, and β-actin were purchased from Cell Signaling Technology (Danvers, MA, USA). All the other chemical agents during the study were of the optimal level commercially available.

Animals and experiments design

Eight-week-old ICR male mice, weighing 22–25 g, were obtained from YISI Experimental Animal Co., Ltd., with a Certificate of Quality No. SCXK (JI) 2016-0003 (Changchun, China). The mice underwent adaptive feeding for at least one week before the formal experiment. The mice were exposed to controlled temperature (22.0 ± 2.0°C) and humidity (60 ± 10%) in a 12 h light/dark pattern in plastic cages and a free supply of food and water. All experimental animal processing procedures were strictly performed according to the Guide for the Care and Use of Laboratory Animals (Ministry of Science and Technology of China, 2016). All animals' protocols were in accordance with the Ethical Committee for Laboratory Animals of Jilin Agricultural University (Permit No.: ECLA-JLAU 2019-00718).

The mice were randomly divided into 4 groups: Normal (N) group (saline for 14 days without HS), HS group (scrotal

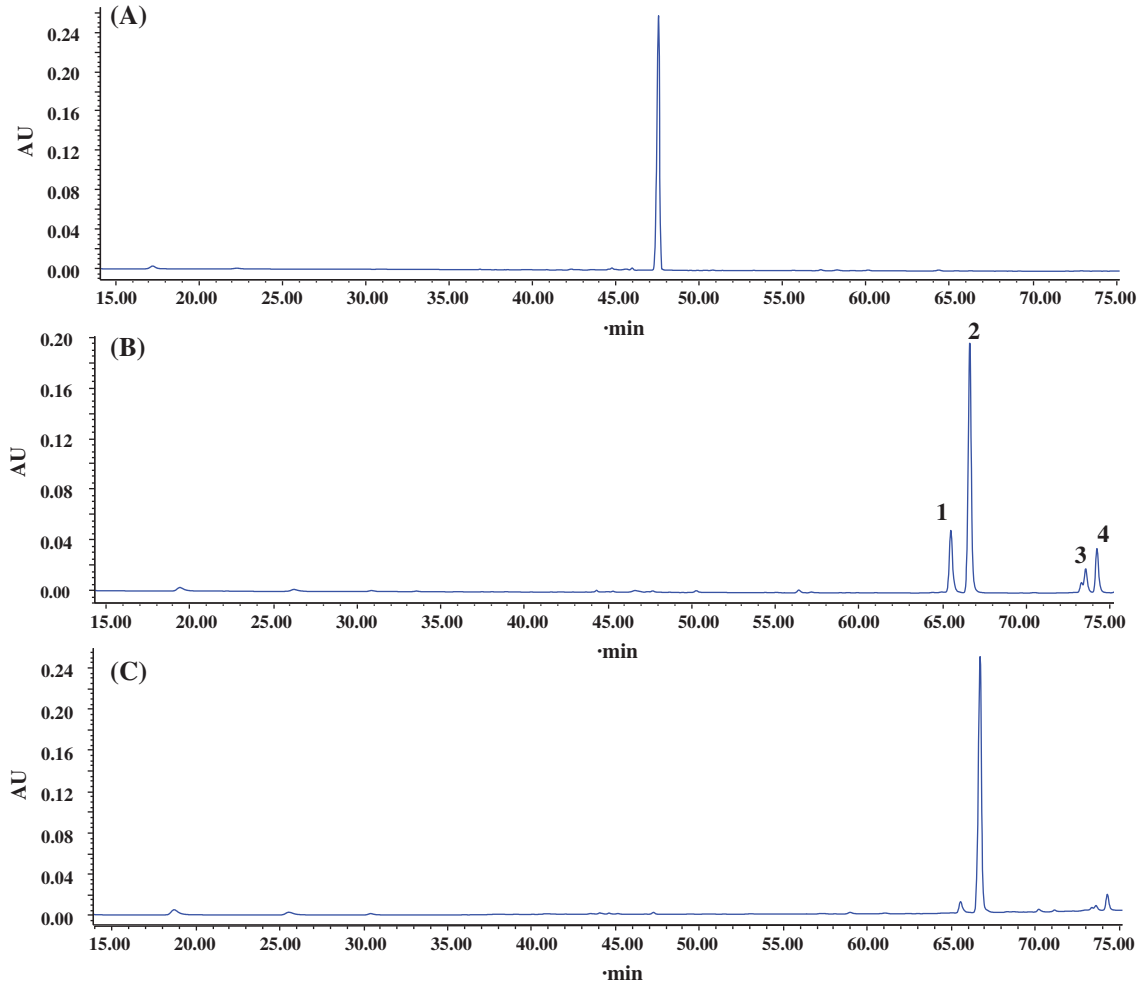

Note:1. 20(S)-Rg3; 2.20(R)-Rg3; 3. Rk1; 4. Rg5

FIGURE 2. HPLC chromatograms of ginsenoside Rd by high-temperature acid treatment and its products. (A) ginsenoside Rd; (B) its high-temperature acid treatment and (C) 20(R)-Rg3.

hyperthermia; 43°C, 18 min), HS + G-Rg3 group (5 mg/kg), and HS + G-Rg3 group (10 mg/kg). Since there is currently no therapeutic agent for scrotal heat-induced spermatogenic damage in the clinic, a group of positive drugs was not set up in the present work. G-Rg3 were dissolved in sodium carboxymethyl cellulose (CMC-Na) to give different doses of 5 and 10 mg/kg according to our previous work and pre-experiments (Zhou *et al.*, 2018), respectively. Mice were administered G-Rg3 orally once daily for 14 days, on the 7th day, all animals except the N groups, other groups were exposed once to HS at 43°C for 18 min to establish a scrotal hyperthermia model as previously described (Leng *et al.*, 2019). For HS treatment, the lower third of the body (hind legs, tail, and scrotum) was submerged in a mini water bath. After 30 min, each animal was dried and returned to its cage. 7 days after HS exposure, the animals were kept in starvation and were euthanized under anesthesia. The testes were excised, weighed, and maintained at −80°C for the subsequent assays.

Determination of serum testosterone levels

Serum was separated from blood after centrifugation (3500 rpm, 10 min) twice at 4°C (Mi *et al.*, 2019). The testosterone level in serum was detected in accordance with the instructions of the commercial kits. Briefly, this kit utilizes the antibodies specific, as well as HRP-conjugated streptavidin solution, to estimate spermatogenic-related products. The absorbance was taken at 450 nm using a MultiskantmTM FC (Thermo Scientific, Waltham, MA, USA).

Estimation of lipid peroxidation

The stored testis was removed from −80°C (frozen tissues within ice-cold phosphate buffer) was comminuted ultrasonically to make tissues homogenate, then centrifuged at 1000×g for 15 min twice and the supernatant was performed to analyze antioxidant activities. The levels of GSH, MDA, and SOD were analyzed by commercial reagent kits according to the manufacturer's protocols. The expressed as MDA (nmol/mg protein) level at 532 nm. GSH (nmol/mg protein) content was monitored at 412 nm, while SOD (U/mg protein) activity was analyzed at 560 nm.

H&E and TUNEL staining

For evaluation of testis and epididymis tissues, which were fixed in a 10% formalin solution for more than 24 h and then embedded in paraffin, both histological and morphometric analyses were performed on 5-μm sections

cut on a rotary microtome. After staining *via* H&E dye kits, subsequently performing an observation histopathological changes used light microscope (Leica, DM750, Germany).

To further evaluate the *in situ* apoptosis in testes, the TUNEL method was performed with apoptosis detection kits (Roche Applied Science, Germany), as previously reported (Xing *et al*., 2019). Briefly, the testis tissue slices were incubated in 20 mg/mL proteinase K solution for 10 min. Pre-equilibrated slices were subsequently incubated with equilibrium buffer solution and terminal deoxynucleotidyl transferase (TdT). Peroxidase activity in each testis section was stained by diaminobenzidine (DAB). Subsequently, apoptotic cells were photographed using a light microscope (Leica TCS SP8, Germany).

Immunohistochemical (IHC) and Immunofluorescence analysis

Immunohistochemical analysis was executed on testis tissue sections as previously described (Li *et al*., 2019). In brief, the 5-μm paraffin sections were de-paraffinized and rehydrated and then treated with citrate buffer solutions (0.01 mol/L, pH 6.0). The slices were incubated chamber overnight at 4°C with primary antibodies. Thereafter, slides were counterstained with hematoxylin staining. Immunostaining was monitored digitalized images snapped with an Olympus camera (Tokyo, Japan).

To assess the expression of HO-1 and HSP70 in HS-induced testicular injury, immunofluorescence staining was exerted in testicular sections of HS-induced groups and N group. Briefly, the sections were rehydrated using xylene and different concentration alcohol solutions, subsequently incubated with primary antibodies overnight at 4°C followed by secondary antibody (BOSTER, Wuhan, China). Then, the sections were further stained with 4,6 diamidino-2-phenylindole (DAPI) (Vector, Burlingame, CA, USA) for 5 min in the dark. Fluorescence microscope (Leica TCS SP8, Germany) and Image-Pro plus 6.0 software were respectively used to observe and analyze the intensity of immunofluorescence staining.

Western blot analysis

The RIPA lysis buffer was used to extract testicular tissue protein and the BCA protein assay kit (NO. P0010S) was used to determine the concentrations of protein (Beyotime, Jiangsu, China). Western blot analysis was performed as our previous research (Ren *et al*., 2019). Then membranes were blocked with 5% BSA for 120 min. Subsequently, the membranes were incubated overnight with primary antibodies at 4°C, the level of β-actin (1:1000) was assessed as a loading control, then the secondary antibody (1:2000) was allowed to bind to the primary antibody for 60 min at room temperature. Signals were captured by Emitter Coupled Logic (ECL) substrate (Pierce Chemical Co., Rockford, IL, USA). The intensities of each band were quantified and analyzed by using the Quantity One software (Bio-Rad Laboratories, Hercules, CA, USA).

Statistical analysis

All data referenced were expressed as the mean ± SD of the indicated number (N) of independent experiments. Differences among experimental groups were performed with one-way analysis of variance (ANOVA) followed by Dunnett's multiple comparison *post hoc* test. Statistical analysis was performed using GraphPad Prism 6.0 software (RRID: SCR_002798, La Jolla California, USA). $p < 0.05$, $p < 0.01$ or $p < 0.001$ were considered significant differences.

Results

G-Rg3 prevented HS-induced changes on testes and epididymis

After administration on the 7th day, the lower body of the mice was placed at 43°C for 18 min to lead to scrotal hyperthermia. The mice were sacrificed 1 week later and immediately measured the weight of the removed testes and epididymis. As showed in Fig. 3A, after HS exposure, the significant shrinkage of testicular and epididymis tissues, and these two organ indices decreased in comparison with the N group ($p < 0.001$). However, G-Rg3 (5 mg/kg) relieved the reduction of testis and epididymis indices. G-Rg3 at high dosage (10 mg/kg) significantly reversed HS-induced these indices decrease ($p < 0.01$, $p < 0.001$). (Figs. 3B–3C).

G-Rg3 prevented HS-induced changes on testes and epididymis

After administration on the 7th day, the lower body of the mice was placed at 43°C for 18 min to lead to scrotal hyperthermia. The mice were sacrificed 1 week later and immediately measured the weight of the removed testes and epididymis. As showed in Fig. 3A, after HS exposure, the significant shrinkage of testicular and epididymis tissues, and these two organ indices decreased in comparison with the N group ($p < 0.001$). However, G-Rg3 (5 mg/kg) relieved the reduction of testis and epididymis indices. G-Rg3 at high dosage (10 mg/kg) significantly reversed HS-induced these indices decrease ($p < 0.01$, $p < 0.001$). (Figs. 3B–3C).

G-Rg3 prevented HS-induced changes on testes and epididymis

After administration on the 7th day, the lower body of the mice was placed at 43°C for 18 min to lead to scrotal hyperthermia. The mice were sacrificed 1 week later and immediately measured the weight of the removed testes and epididymis. As showed in Fig. 3A, after HS exposure, the significant shrinkage of testicular and epididymis tissues, and these two organ indices decreased in comparison with the N group ($p < 0.001$). However, G-Rg3 (5 mg/kg) relieved the reduction of testis and epididymis indices. G-Rg3 at high dosage (10 mg/kg) significantly reversed HS-induced these indices decrease ($p < 0.01$, $p < 0.001$). (Figs. 3B–3C).

G-Rg3 ameliorated HS-induced histopathological alterations

Histologically, testicular tissues from mice in the N group showed quite normal with dynamic spermatogenesis (Fig. 3D). Contrary, a single treatment of HS caused severe damage to spermatogenic cells, with vacuolated nuclei less larges primary spermatocytes and absence of sperm formation, atrophic seminiferous epithelium cells appear to be degeneration, vacuolization, and disorganization. Interestingly, all the testicular structure and seminiferous

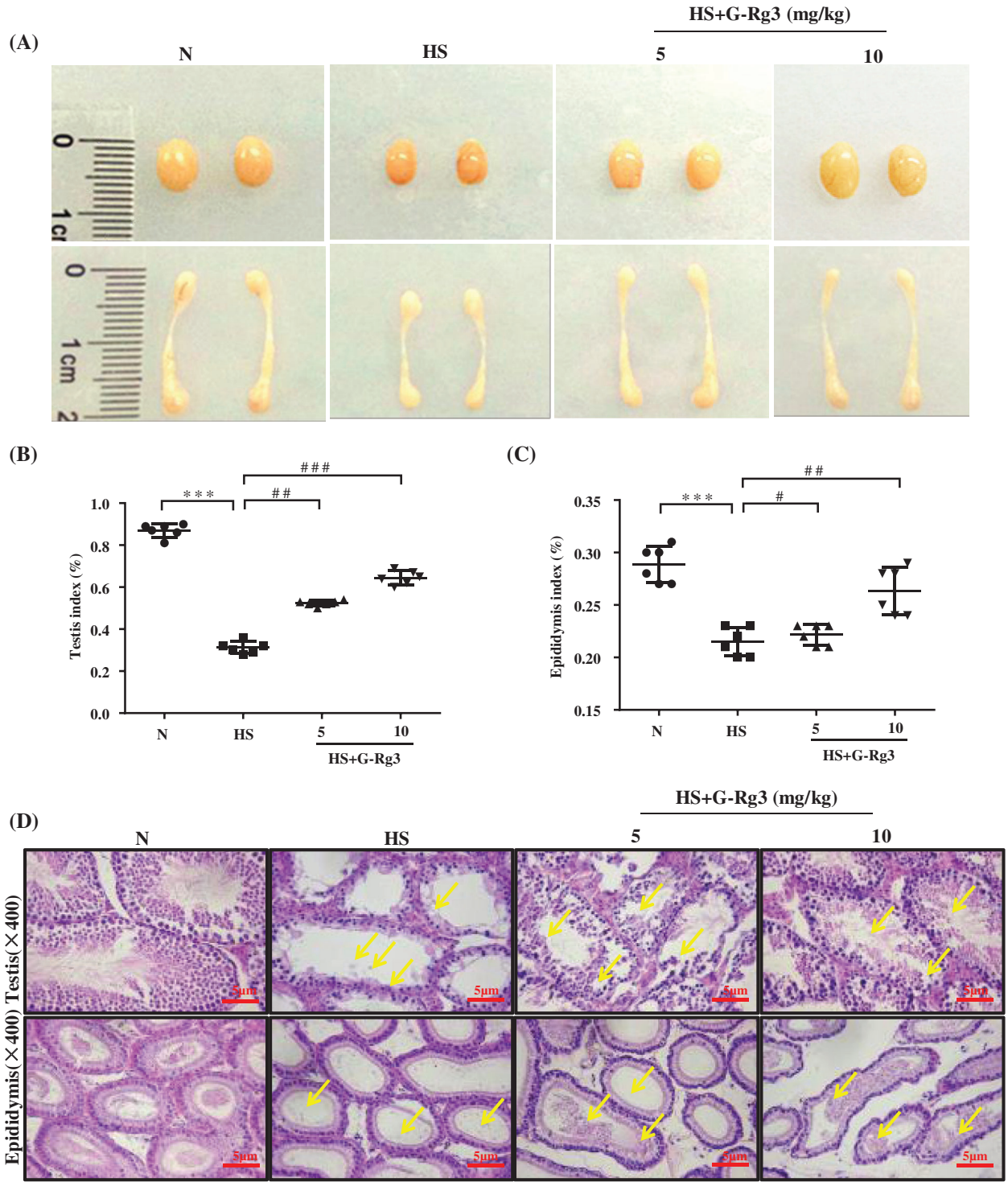

FIGURE 3. Effects of G-Rg3 on changes of organ indices and histopathological characteristic in HS mice. (A) Testis and epididymis histomorphology; (B) Testis indices; (C) Epididymis indices; (D) H&E staining was used for analysis of histological abnormalities in testis and epididymis tissue (N = 6 each group). Data are expressed as mean ± SD. $^{**}p < 0.01$, $^{***}p < 0.001$ vs. N group; $^{\#}p < 0.05$, $^{\#\#}p < 0.01$ and $^{\#\#\#}p < 0.001$ *vs.* HS group.

tubules were almost completely restored to a normal level by G-Rg3 treatment, especially at a high dosage of 10 mg/kg.

G-Rg3 reversed HS-induced testosterone concentration

Testosterone is an important indicator to evaluate male testicular function. Simultaneously, also as a biomarker for spermatogenesis and sperm maturation (Wang *et al.*, 2009). As shown in Fig. 4A, the serum testosterone concentration of the HS group was significantly lower than the N group ($p < 0.05$). Treatment with two different doses of G-Rg3 for two weeks significantly enhanced the testosterone level ($p < 0.01$).

G-Rg3 inhibited HS-induced oxidative stress injury

Oxidative damage is one of the key indicators in the evaluation of HS-treated mice, since SOD and GSH are free radical scavengers and good antioxidants, and we investigated whether G-Rg3 treatment could regulate airframe antioxidant activity. As shown in Figs. 4B–4D, the

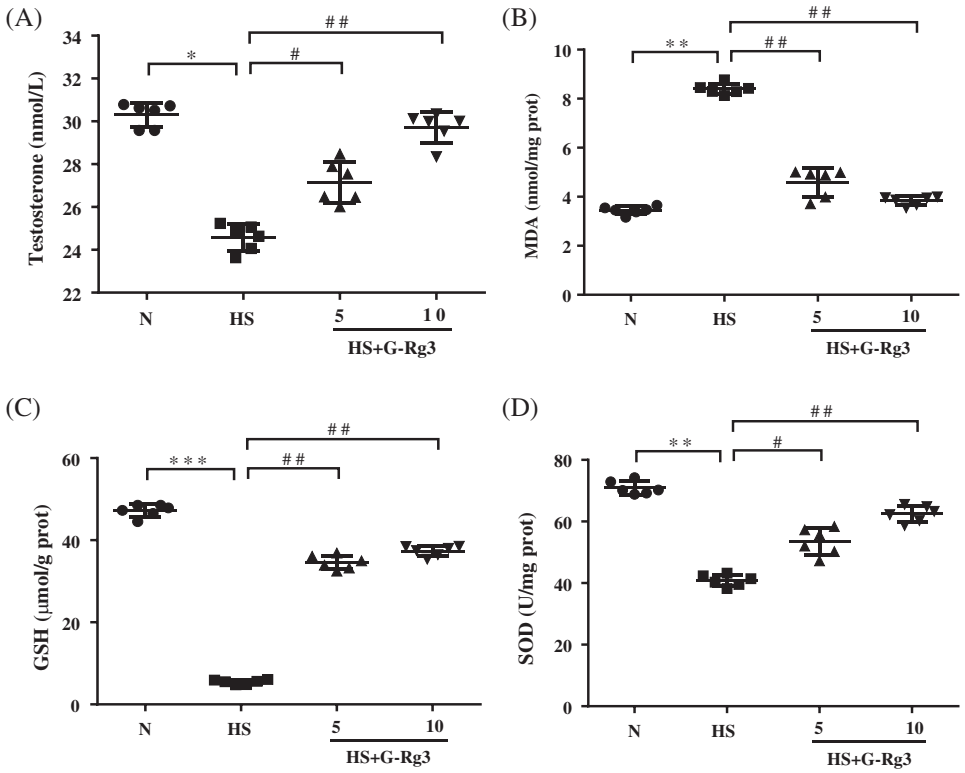

FIGURE 4. G-Rg3 regulated spermatogenic-related and oxidative stress parameters in HS mice. (A) Concentration of serum testosterone; (B) MDA level; (C) GSH content; (D) SOD activity in testis tissues (N = 6 each group). Data are expressed as mean ± SD. $^{*}p < 0.05$ $^{**}p < 0.01$ and $^{***}p < 0.001$ *vs.* N group; $^{\#}p < 0.05$, $^{\#\#}p < 0.01$ *vs.* HS group.

levels of GSH and SOD in the testis homogenate of the HS group were significantly lower than those of the N group ($p < 0.001$), while the G-Rg3 treatment at the dose of 5 and 10 mg/kg inhibited the decrease of GSH and SOD levels to varying degrees ($p < 0.01$). Meanwhile, G-Rg3 significantly inhibited HS-induced MDA elevation ($p < 0.05$, $p < 0.01$).

In order to further confirm the generation of oxidative stress *in vivo*, immunofluorescence (Figs. 5A–5D) was employed to confirm the expression of HO-1 and HSP70 in testis tissues. The HS group showed the overexpression of these protein levels ($p < 0.01$), and treatment with G-Rg3 significantly attenuated at both 5 mg/kg and 10 mg/kg, respectively ($p < 0.05$, $p < 0.01$).

Additionally, the expression levels of oxidation-related protein (HIF-1α, HO-1, HSP-70) also significantly reduced ($p < 0.01$) in the HS group. Band intensities revealed clearly after G-Rg3 (5 and 10 mg/kg) treatment for two weeks remarkably elevated ($p < 0.05$, $p < 0.01$) (Figs. 5E–5H).

G-Rg3 alleviated HS-stimulated apoptosis

In order to verify whether HS-induced spermatogenic damage was associated with apoptosis, TUNEL staining was used to observe the changes in nuclear morphology. As shown in Figs. 6A, 6B, clear and large brown color staining of the nucleus was discovered around the sperm cells in the testes of the HS group. Upon exposure of the testis to HS, the nuclear chromatin weakly and seriously affects spermatogenesis. In contrast, the number of TUNEL-positive cells was extremely reduced by G-Rg3 pre-treatment. Preliminary evidence showed that G-Rg3 exerted anti-apoptotic effects in HS-induced damage ($p < 0.01$).

Additionally, the results of immunohistochemistry also showed that the evidently reduced the expression of Bcl-2 and elevated the expression of Bax by HS-induced spermatogenic cellular apoptosis (Figs. 6C–6E). However, these changes could be significantly mitigated by G-Rg3 treatment ($p < 0.05$, $p < 0.01$).

Furthermore, we further examined the expression levels of apoptotic protein in testis tissues by western blot analysis. As shown in Figs. 6F–6J, HS exposure increased the protein level of Bax and reduced the expressions of Bcl-2 and Bcl-XL in the testis tissues, respectively ($p < 0.01$). But the decrease of Bax ($p < 0.01$) was simultaneously attenuated by supplement with G-Rg3 on the 14th day, while significantly improved the protein Bcl-2 and Bcl-XL expression ($p < 0.01$). These findings fully demonstrate that G-Rg3 treatment prevented HS-induced testicular tissue apoptosis.

G-Rg3 regulated the MAPK signaling pathways

In the present study, we detected the expression of MAPK family members by western blot analysis and explore the underlying mechanism of G-Rg3 on HS-induced spermatogenesis disorders in mice. As shown in Figs. 7A–7C, the expressions of JNK, ERK and p38 MAPK phosphorylation proteins increased ($p < 0.01$) in the mice of HS group. However, the effect of G-Rg3 was the most significantly at high dosage of 10 mg/kg ($p < 0.01$). These results indicated that the protective effects of G-Rg3 treatment on HS-induced spermatogenesis disorders is closely related to the MAPK signaling pathway.

Discussion

With the changes in climatic conditions and living environment, a series of diseases caused by HS is gradually gaining importance (Dahl *et al.*, 2019). A growing body of

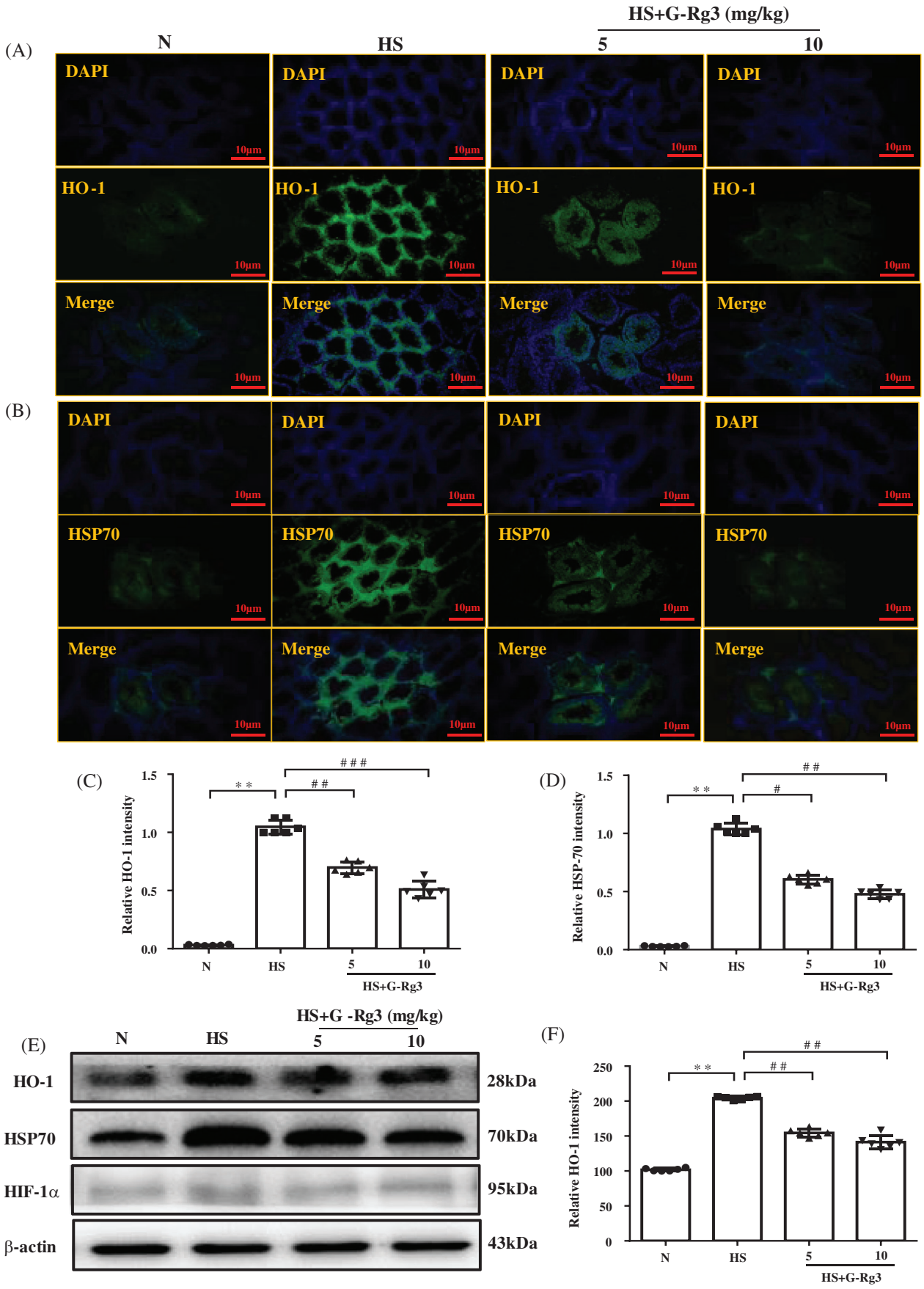

FIGURE 5. (continued)

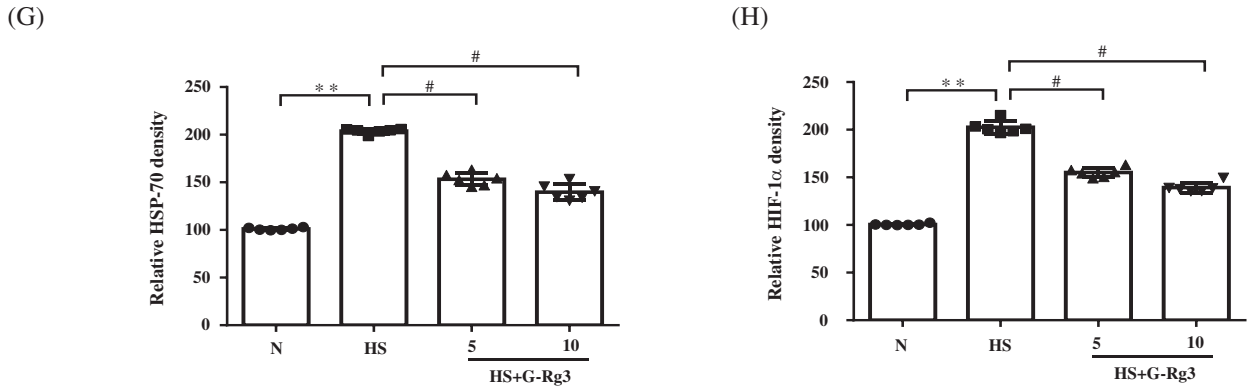

FIGURE 5. Administration with G-Rg3 inhibited the expression of oxidative stress-related protein induced by HS. (A-B) Testis tissues (5-μm section) from each group were processed for anti-HO-1 and anti-HSP-70 immunofluorescence staining as described in materials and methods; Representative staining images were shown (magnification ×200). (C-D) The HO-1 and HSP-70 (green) quantitation of fluorescence intensities; (E) Western blot analysis of oxidative stress-related (HO-1, HSP70 and HIF-1α). Tissues were homogenized and processed into western blot analysis of these protein expressions, and β-actin, as loading control; (F-H) Quantification of relative protein expression were performed by densitometric analysis (N = 6 each group). Data are expressed as mean ± SD. $^{**}p < 0.01$ *vs*. N group; $^{\#}p < 0.05$, $^{\#\#}p < 0.01$ and $^{\#\#\#}p < 0.01$ *vs*. HS group.

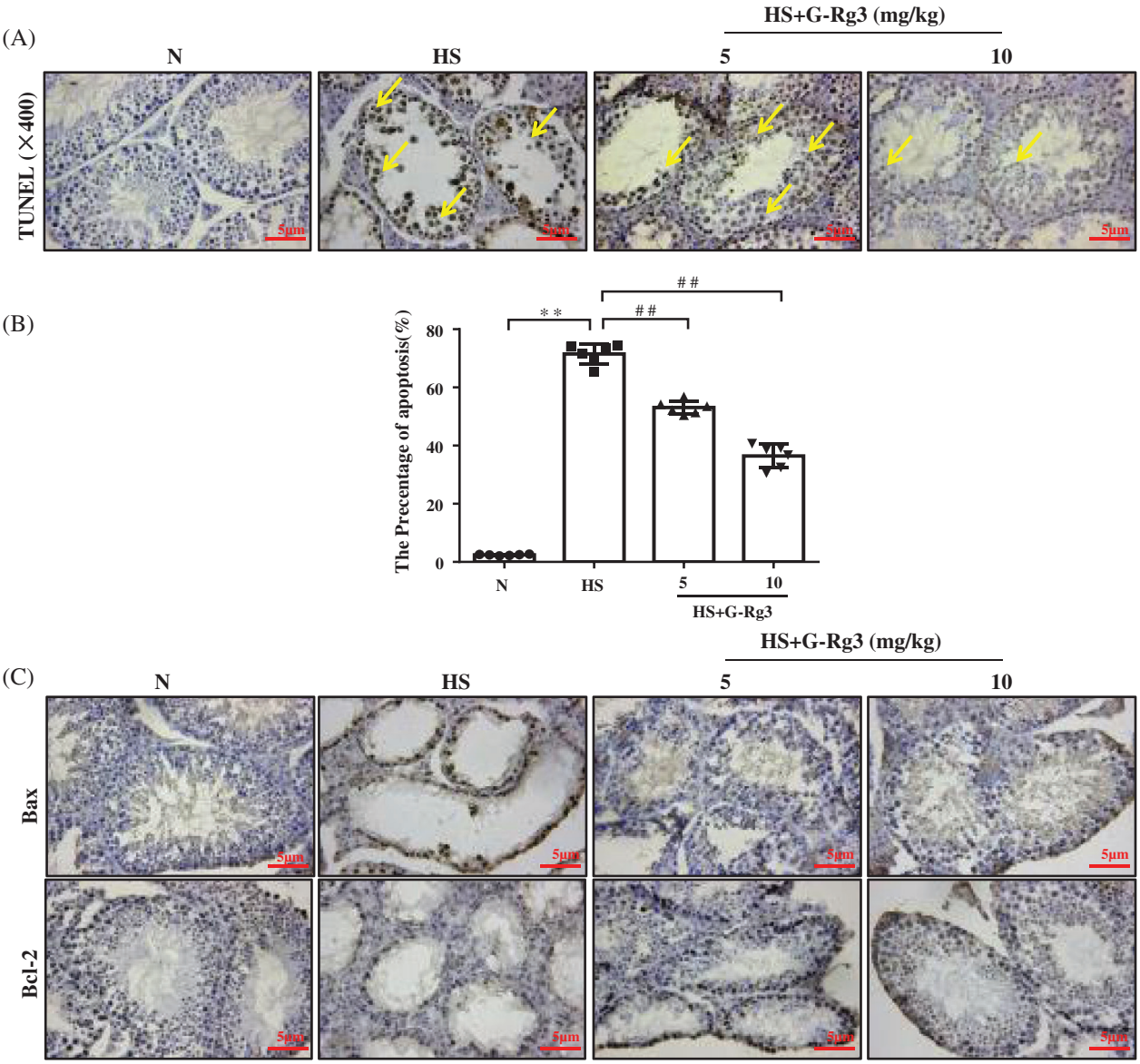

FIGURE 6. (continued)

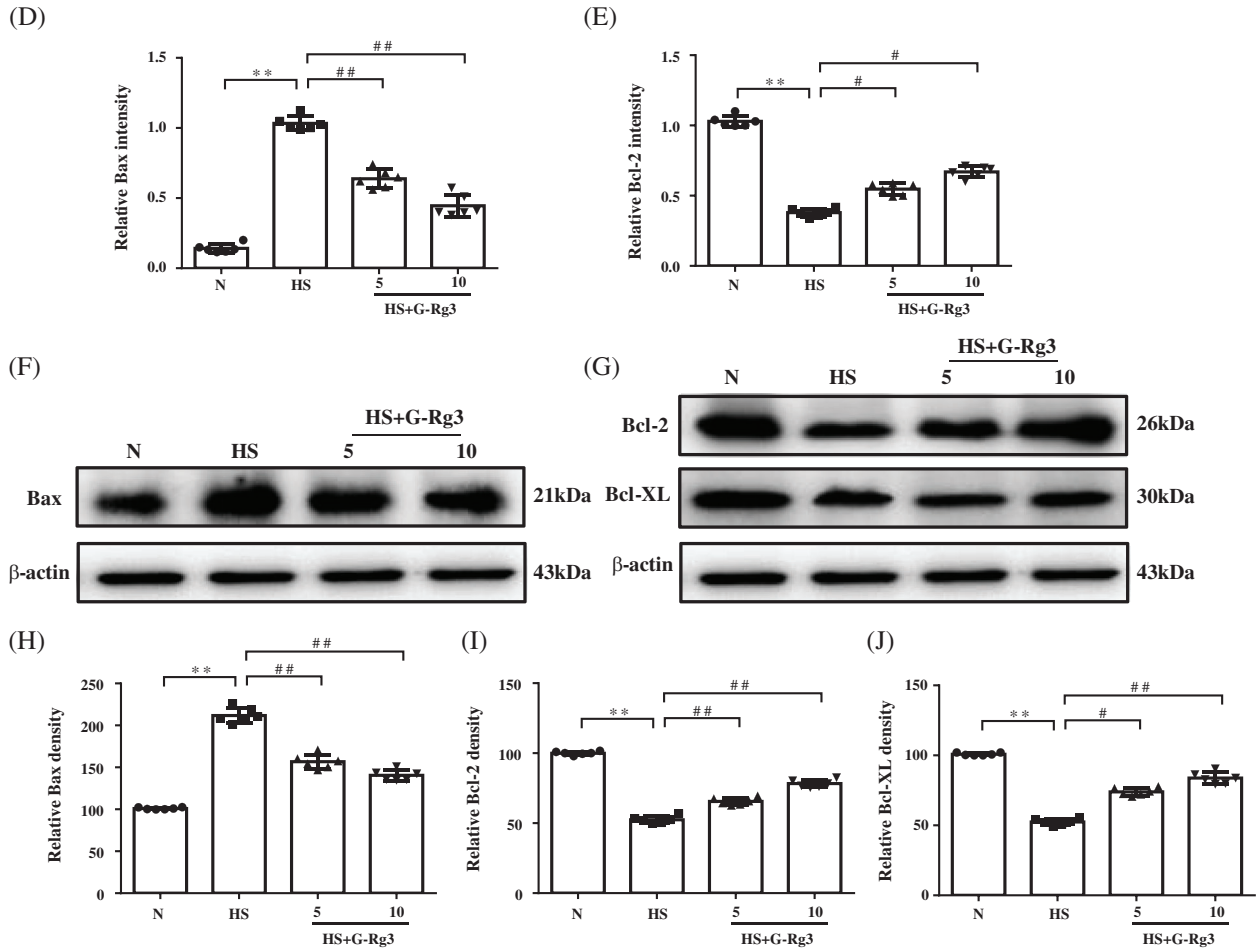

FIGURE 6. G-Rg3 regulated on apoptosis in HS mice and inhibited the expression of apoptosis-related protein induced by HS. (A) TUNEL assay of apoptotic spermatogenic cell; (B) Quantitative analysis of TUNEL-positive cell; (C) Testis tissues (5-μm section) from each group were processed for Bax and Bcl-2 immunohistochemical staining as described in materials and methods; Representative staining images were shown (magnification ×400); (D-E) Quantitative analysis of Bax and Bcl-2 positive cells; (F) Western blot analysis of apoptosis-related (Bax, Bcl-2 and Bcl-XL). Tissues were homogenized and processed into western blot analysis of these protein expressions, and β-actin protein was used as loading control; (G-J) Quantification of relative protein expression was performed by densitometric analysis (N = 6 each group). Data are expressed as mean ± SD. $^{**}p < 0.01$ *vs.* N group; $^{\#}p < 0.05$, $^{\#\#}p < 0.01$ and $^{\#\#\#}p < 0.001$ *vs.* HS group.

evidence indicates that HS-induced by high-temperature results in deleterious effects such as high blood pressure, cardiac (Chen *et al.*, 2020), gastric mucosa lesions (Qin *et al.*, 2007), and multiorgan dysfunction (Havenith *et al.*, 1995) in human. However, it is worth noting that spermatogenesis is a temperature-dependent process and that scrotal temperature is one of the most important causes of impaired spermatogenesis and male infertility (Liu *et al.*, 2016; Rao *et al.*, 2015). Therefore, it is important to prevent an elevated temperature in testis caused by external environmental factors. In the present study, the protective effects of G-Rg3 against HS-induced testicular damage were investigated in male mice. HS can cause a decrease in the testis and epididymis indices and morphological atrophy and lead to oxidative stress injury and spermatogenic cell apoptosis. Our results showed that G-Rg3 treatment (5 and 10 mg/kg) for consecutive two weeks improved changes in basic indicators and inhibited the expression level of oxidized and apoptosis proteins and were related to the activation of MAPK signaling pathways.

More and more evidence showed that dietary medicinal food has beneficial effects on health, especially under HS. *P. ginseng* has gained its popularity as an adaptogen for thousand years due to its triterpenoid saponins (call ginsenosides). These ginsenosides are unique and classified, has numerous powerful pharmacological effects, such as on the central nervous system, endocrine, immunomodulatory, and cardiovascular systems (Lee *et al.*, 2019; Qi *et al.*, 2011). PPD-type ginsenosides are the most enriching saponins in Asian ginseng and American ginseng, including ginsenosides Rb1, Rc, Rb2, and Rd, whereas ginsenoside Rg3 is abundantly present in Red or Black ginseng. More importantly, deglycosylation and dehydration reactions of glycosylation of C-3 and C-20 hydroxyl groups by heat processing, acid treatment or biotransformation, can production of rare saponins, such as ginsenoside Rg3, Rk1, Rg5, F2, and Compound K, etc. These transformed ginsenosides further contribute to the chemical and pharmacological activity diversity of ginsenosides. In this study, a rare saponin G-Rg3 was prepared by using PPD-type ginsenoside Rd as a reaction substrate and used to investigate the protective effect of scrotal HS-induced on spermatogenic damage. Based on previous studies found that G-Rg3 has multiple

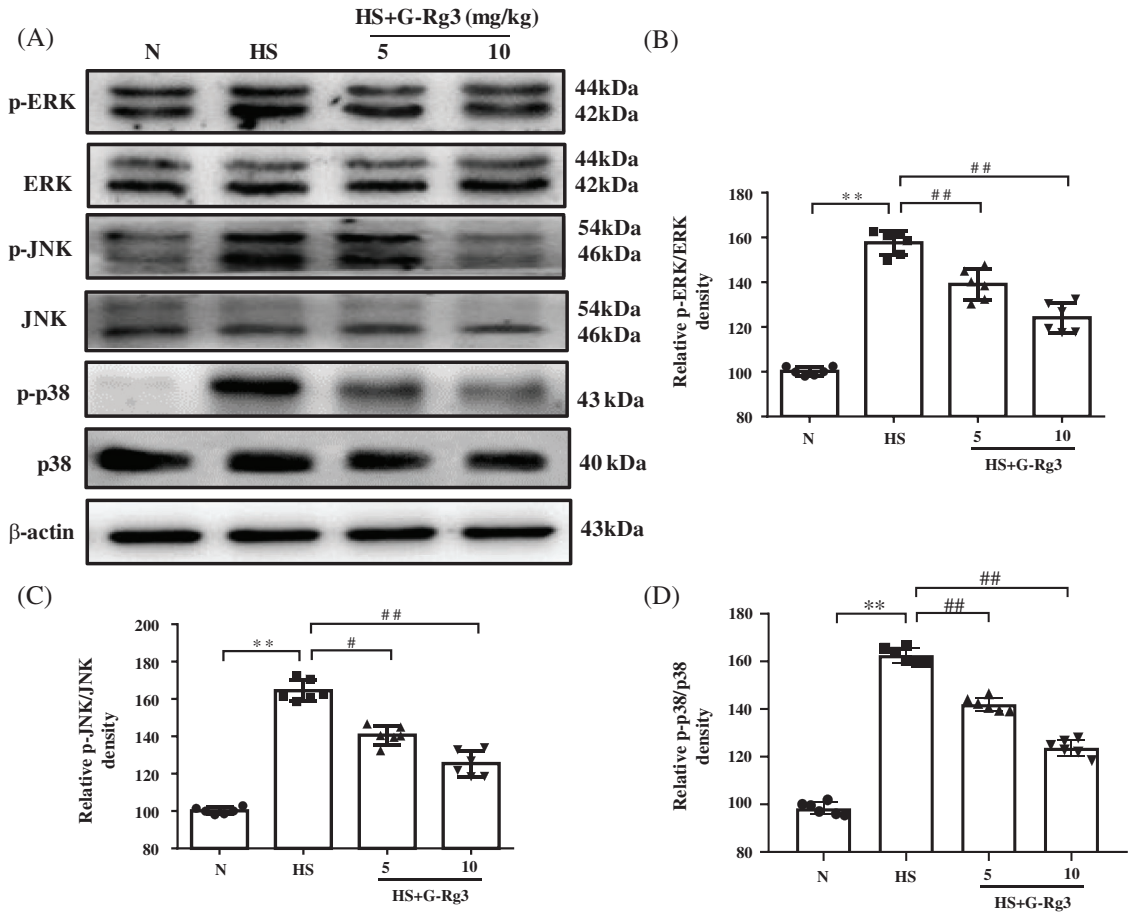

FIGURE 7. Administration with G-Rg3 regulated MAPK signaling pathway induced by HS. (A) Western blot analysis of MAPKs. Tissues were homogenized and processed into western blot analysis of ERK, JNK, p38 MAPK, and their phosphorylated forms, and β-actin as loading control; (B-D) Quantification of relative protein expression was performed by densitometric analysis (N = 6 each group). Data are expressed as mean ± SD. $^{**}p < 0.01$ *vs.* N group; $^{\#}p < 0.05$, $^{\#\#}p < 0.01$ *vs.* HS group.

beneficial effects in acute experimental animal models (Zhou *et al.*, 2018).

Recent studies on various animal tissues and experimental models have indicated that HS can severely and adversely affect the isolation of spermatogenic cells by disrupting spermatogenesis and altering oxidative metabolism (Ghasemi *et al.*, 2009). Prior to the present study, Kopalli *et al.* (Kopalli *et al.*, 2019) have confirmed that Korean red ginseng extract (enriched ginsenoside Rg3) protects the scrotal from chronic intermittent HS-induced spermatogenic damage and help to recover testicular function by restoring intrinsic anti-oxidant defenses. Similarly, in the current histopathological examination of tissues, the slides stained with H&E revealed disordered seminiferous tubules and spermatocytes and spermatids severe lesions or even disappeared in the HS group. However, supplement with G-Rg3 restored HS-induced tissue damage with varying degrees, especially the 10 mg/kg of G-Rg3 almost full recovery.

Meantime, HS-induced oxidative stress is mainly caused by lipid peroxidation of cell membrane potential, intracellular ROS, and MDA concentrations in the testes, which can be closely related to the degree of membrane system damage (Li *et al.*, 2014). Recent research has also illustrated that hypoxia stress, such as HS, causes a rapid increase of ROS, and is correlated with the upregulation of the SOD and GSH (Kim *et al.*, 2013a). More importantly, antioxidant enzymes also limit the toxicity associated with free radicals or ROS, which disturb the balance of redox reaction *in vivo* (Li *et al.*, 2018). In the current work, the MDA level expression in the HS group was significantly increased with compared to the N group, and our experimental data showed that G-Rg3 treatment (5 and 10 mg/kg) for consecutive two weeks reversed elevation of MDA, as well as reduction of GSH and SOD in the testis.

Apart from these biochemical parameters, it is worth noting that HO-1 and HSP-70 are the most important cytokines for evaluating peroxidative damage (Farag *et al.*, 2019). Evidence also suggests that HIF-1α is currently the single most important indicator of impaired testicular function, which is a central regulator responsible for the regulation of pathological inducible response (Li *et al.*, 2017). In agreement, our present study showed a significant reduction in the expression of antioxidative proteins related to spermatogenesis such as HO-1, HSP-70, and HIF-1α levels in HS groups, and treatment with G-Rg3 significantly ameliorated these changes by immunofluorescence staining and western blot analysis. Collectively, these results provide more strong evidence that G-Rg3 may in preventing HS-induced oxidative damage in the mice testis.

Importantly, there are few studies on the specific mechanism of HS-induced spermatogenic damage. MAPKs

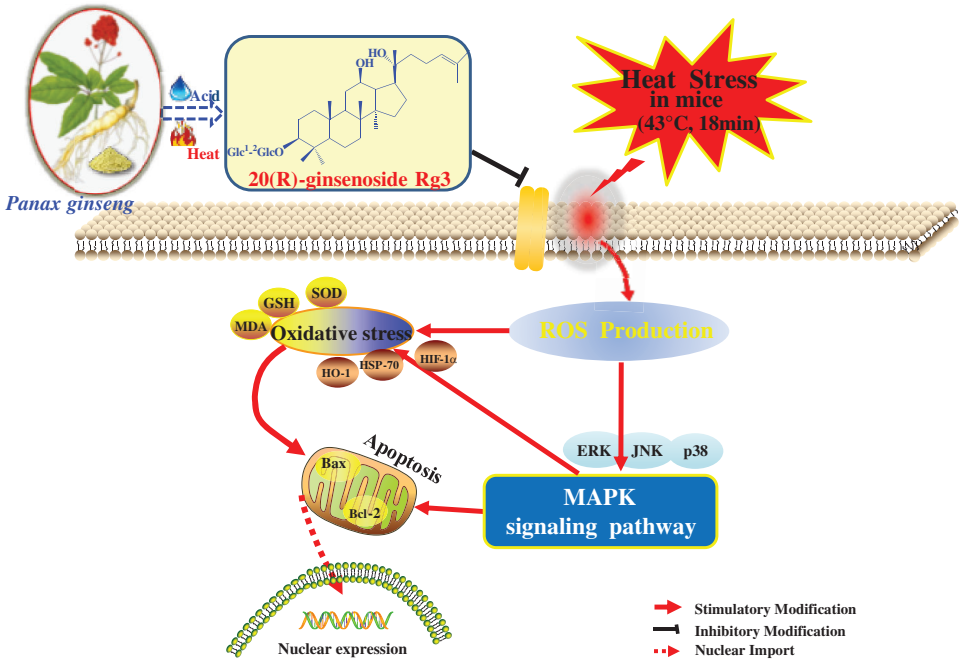

FIGURE 8. Proposed mechanisms of G-Rg3 mediated protection to scrotal heat stress in mice.

is known to play a critical role in the signal cellular programs of transduction, and also throughout evolution in many physiological processes (M and Pp, 2011), JNK, ERK, and p38 are important proteins of the MAPK family, engages in cytokine synthesis and differentiation, especially closely related to the production of ROS and oxidative stress (Azadeh *et al.*, 2020). Activated MAPK also can regulate cell growth, motility, and mitochondrial pathway-mediated apoptosis (Sui *et al.*, 2014). Thus, we speculate that the MAPK signaling pathway may be involved in regulating oxidative stress and apoptosis induced by HS. In current experiments, HS exposure increased the protein expression levels of JNK, ERK, and p38 in testis tissues. However, G-Rg3 treatment significantly reduced the expression of these proteins. The present study confirmed the negative regulation of G-Rg3 on the MAPK signaling pathway (Fig. 8).

Mounting evidence suggests that MAPK can alter various oxidative enzymes and involved mitochondrial-induced apoptosis, and the expression of Bax and Bcl-2 apoptosis proteins is also closely related to JNK phosphorylation (Ki *et al.*, 2013). Meantime, previous studies have confirmed that experimental cryptorchidism can also cause apoptosis (Shikone *et al.*, 1994). As showed in this experiment, our data demonstrated that G-Rg3 treatment ameliorates the expressions of effector Bax, Bcl-2, and Bcl-XL, showing that G-Rg3 has a great anti-apoptotic activity to relieve HS-induced germ cell apoptosis. Furthermore, cell apoptosis in *vivo* is quite complicated and can be regulated by interacting with one another through various mechanisms (Sinha Hikim *et al.*, 2003). In the current study, TUNEL assay and immunohistochemical staining also verified the anti-apoptotic effect of G-Rg3. However, it is worth noting that organ damages induced by HS, may be regulated by complex signal pathways and various other factors in *vivo*. The protective effects of G-Rg3 on the male testis under HS conditions need further investigations both in *vivo* and in *vitro*.

In conclusion, this research used the efficient thermal deglycosylation of ginsenoside Rd to prepared G-Rg3 and further demonstrated that the protective effects and underlying mechanism of G-Rg3 against HS-induced spermatogenic damage in mice by suppression of ROS-mediated oxidative stress and apoptosis *via* partly regulation of the MAPK signaling pathway. G-Rg3 can be an important natural ingredient, which has potential therapeutic for the clinical treatment of male infertility or infertility caused by hyperthermia.

Availability of Data and Materials: The data used to support the findings of this study are available from the corresponding author upon request.

Funding Statement: This work was supported by the grants of the Jilin Science & Technology Development Plan (Nos. 20170101011JC, 20200301037RQ and 20190103092JH) and the Open Fund of Key Laboratory of Biotechnology and Bioresources Utilization (KF202004).

Conflict of Interest: The authors declare that there are no conflicts of interest.

References

Agarwal A, Mulgund A, Hamada A, Chyatte MR (2015). A unique view on male infertility around the globe. *Reproductive Biology and Endocrinology* **13**: 837. DOI 10.1186/s12958-015-0032-1.

Aitken RJ, Clarkson JS (1987). Cellular basis of defective sperm function and its association with the genesis of reactive oxygen species by human spermatozoa. *Reproduction* **81**: 459–469. DOI 10.1530/jrf.0.0810459.

Azadeh A, Neda TM, Mehrnaz M, Kobra BJ, Sharifi AM (2020). Investigating The Alterations of Oxidative Stress Status, Antioxidant Defense Mechanisms, MAP Kinase and Mitochondrial Apoptotic Pathway in Adipose-Derived Mesenchymal Stem Cells from STZ Diabetic Rats. *Cell Journal* **22**: 38–48. DOI 10.22074/cellj.2020.6958.

Baird NA, Turnbull DW, Johnson EA (2006). Induction of the heat shock pathway during hypoxia requires regulation of heat shock factor by hypoxia-inducible factor-1. *Journal of Biological Chemistry* **281**: 38675–38681. DOI 10.1074/jbc.M608013200.

Bromfield EG, Aitken RJ, Mclaughlin EA, Nixon B (2016). Proteolytic degradation of heat shock protein A2 occurs in response to oxidative stress in male germ cells of the mouse. *Molecular Human Reproduction* **13**: 26–105. DOI 10.1093/molehr/gaw074.

Cai H, Ren Y, Li XX, Yang JL, Zhang CP, Chen M, Fan CH, Hu XQ, Hu ZY, Gao F, Liu YX (2011). Scrotal heat stress causes a transient alteration in tight junctions and induction of TGF-beta expression. *International Journal of Andrology* **34**: 352–362. DOI 10.1111/j.1365-2605.2010.01089.x.

Castillo J, Bogle OA, Jodar M, Torabi F, Delgado-Duenas D, Estanyol JM, Ballesca JL, Miller D, Oliva R (2019). Proteomic changes in human sperm during sequential *in vitro* capacitation and acrosome reaction. *Frontiers in Cell and Developmental Biology* **7**: 40. DOI 10.3389/fcell.2019.00295.

Costa GMJ, Lacerda S, Figueiredo AFA, Leal MC, Rezende-Neto JV, Franca LR (2018). Higher environmental temperatures promote acceleration of spermatogenesis *in vivo* in mice (*Mus musculus*). *Journal of Thermal Biology* **77**: 14–23. DOI 10.1016/j.jtherbio.2018.07.010.

Chen Y, Jiang W, Liu X, Du Y, Liu L, Ordovas JM, Lai CQ, Shen L (2020). Curcumin supplementation improves heat-stress-induced cardiac injury of mice: physiological and molecular mechanisms. *Journal of Nutritional Biochemistry* **78**: 108331. DOI 10.1016/j.jnutbio.2019.108331.

Dahl GE, Skibiel AL, Laporta J (2019). *In utero* heat stress programs reduced performance and health in calves. *Veterinary Clinics of North America: Food Animal Practice* **35**: 343–353. DOI 10.1016/j.cvfa.2019.02.005.

De Blois J, Kjellstrom T, Agewall S, Ezekowitz JA, Armstrong PW, Atar D (2015). The effects of climate change on cardiac health. *Cardiology* **131**: 209–217. DOI 10.1159/000398787.

Durairajanayagam D, Agarwal A, Ong C (2015). Causes, effects and molecular mechanisms of testicular heat stress. *Reproductive BioMedicine Online* **30**: 14–27. DOI 10.1016/j.rbmo.2014.09.018.

Fan HY (2020). Regioselective synthesis and structures of anti-cancer 20(R)-ginsenoside Rg_3 derivatives. *Natural Product Research* **34**: 1962–1970. DOI 10.1080/14786419.2019.1569007.

Farag MR, Elhady WM, Ahmed SYA, Taha HSA, Alagawany M (2019). Astragalus polysaccharides alleviate tilmicosin-induced toxicity in rats by inhibiting oxidative damage and modulating the expressions of HSP70, NF-kB and Nrf2/HO-1 pathway. *Research in Veterinary Science* **124**: 137–148. DOI 10.1016/j.rvsc.2019.03.010.

Fischer U, Schulze-Osthoff K (2005). Apoptosis-based therapies and drug targets. *Cell Death & Differentiation* **12**: 942–961. DOI 10.1038/sj.cdd.4401556.

Ghasemi N, Babaei H, Azizallahi S, Kheradmand A (2009). Effect of long-term administration of zinc after scrotal heating on mice spermatozoa and subsequent offspring quality. *Andrologia* **41**: 222–228. DOI 10.1111/j.1439-0272.2009.00920.x.

Han J, Shao J, Chen Q, Sun H, Guan L, Li Y, Liu J, Liu H (2019). Transcriptional changes in the hypothalamus, pituitary, and mammary gland underlying decreased lactation performance in mice under heat stress. *FASEB Journal* **33**: 12588–12601. DOI 10.1096/fj.201901045R.

Havenith G, Luttikholt VG, Vrijkotte TG (1995). The relative influence of body characteristics on humid heat stress response. *European Journal of Applied Physiology and Occupational Physiology* **70**: 270–279. DOI 10.1007/BF00238575.

Houston BJ, Nixon B, Martin JH, De Iuliis GN, Trigg NA, Bromfield EG, Mcewan KE, Aitken RJ (2018). Heat exposure induces oxidative stress and DNA damage in the male germ line. *Biology of Reproduction* **98**: 593–606. DOI 10.1093/biolre/ioy009.

Hu Y, Wang Y, Yan T, Feng D, Ba Y, Zhang H, Zhu J, Cheng X, Cui L, Huang H (2019). N-acetylcysteine alleviates fluoride-induced testicular apoptosis by modulating IRE1α/JNK signaling and nuclear Nrf2 activation. *Reproductive Toxicology* **84**: 98–107. DOI 10.1016/j.reprotox.2019.01.001.

Hughes IA, Acerini CL (2008). Factors controlling testis descent. *European Journal of Endocrinology* **159**: S75–S82. DOI 10.1530/EJE-08-0458.

Jin Y, Kim YJ, Jeon JN, Wang C, Min JW, Noh HY, Yang DC (2015). Effect of white, red and black ginseng on physicochemical properties and ginsenosides. *Plant Foods for Human Nutrition* **70**: 141–145. DOI 10.1007/s11130-015-0470-0.

Kheradmand A, Dezfoulian O, Alirezaei M (2012). Ghrelin regulates Bax and PCNA but not Bcl-2 expressions following scrotal hyperthermia in the rat. *Tissue and Cell* **44**: 308–315. DOI 10.1016/j.tice.2012.04.009.

Ki YW, Park JH, Lee JE, Shin IC, Koh HC (2013). JNK and p38 MAPK regulate oxidative stress and the inflammatory response in chlorpyrifos-induced apoptosis. *Toxicology Letters* **218**: 235–245. DOI 10.1016/j.toxlet.2013.02.003.

Kim B, Park K, Rhee K (2013a). Heat stress response of male germ cells. *Cellular and Molecular Life Sciences* **70**: 2623–2636. DOI 10.1007/s00018-012-1165-4.

Kim JC, Jeon JY, Yang WS, Kim CH, Eom DW (2019). Combined amelioration of ginsenoside (Rg1, Rb1, and Rg3)-enriched Korean red ginseng and probiotic *Lactobacillus* on non-alcoholic fatty liver disease. *Current Pharmaceutical Biotechnology* **20**: 222–231. DOI 10.2174/1389201020666190311143554.

Kim K, Nam KH, Yi SA, Park JW, Han JW, Lee J (2020). Ginsenoside Rg3 induces browning of 3T3-L1 adipocytes by activating AMPK signaling. *Nutrients* **12**: 427. DOI 10.3390/nu12020427.

Kim KJ, Yoon KY, Hong HD, Lee BY (2015). Role of the red ginseng in defense against the environmental heat stress in Sprague Dawley rats. *Molecules* **20**: 20240–20253. DOI 10.3390/molecules201119692.

Kim YJ, Yamabe N, Choi P, Lee JW, Ham J, Kang KS (2013b). Efficient thermal deglycosylation of ginsenoside Rd and its contribution to the improved anticancer activity of ginseng. *Journal of Agricultural and Food Chemistry* **61**: 9185–9191. DOI 10.1021/jf402774d.

Kopalli SR, Cha KM, Hwang SY, Jeong MS, Kim SK (2019). Korean red ginseng (*Panax ginseng* Meyer) with enriched Rg3 ameliorates chronic intermittent heat stress-induced testicular damage in rats via multifunctional approach. *Journal of Ginseng Research* **43**: 135–142. DOI 10.1016/j.jgr.2018.06.004.

Lee SM, Shon HJ, Choi CS, Hung TM, Min BS, Bie KH (2009). Ginsenosides from Heat Processed Ginseng. *Chemical & Pharmaceutical Bulletin* **57**: 92–94. DOI 10.1248/cpb.57.92.

Lee IS, Kang KS, Kim SY (2020). *Panax ginseng* pharmacopuncture: Current status of the research and future challenges. *Biomolecules* **10**: 33. DOI 10.3390/biom10010033.

Leng J, Hou JG, Fu CL, Ren S, Jiang S, Wang YP, Chen C, Wang Z, Li W (2019). Platycodon grandiflorum Saponins attenuate scrotal heat-induced spermatogenic damage via inhibition of oxidative stress and apoptosis in mice. *Journal of Functional Foods* **54**: 479–488. DOI 10.1016/j.jff.2019.01.050.

Li D, Du Y, Yuan X, Han X, Dong Z, Chen X, Wu H, Zhang J, Xu L, Han C, Zhang M, Xia Q (2017). Hepatic hypoxia-inducible factors inhibit PPARα expression to exacerbate acetaminophen induced oxidative stress and hepatotoxicity. *Free Radical Biology and Medicine* **110**: 102–116. DOI 10.1016/j.freeradbiomed.2017.06.002.

Li RY, Zhang WZ, Yan XT, Hou JG, Wang Z, Ding CB, Liu WC, Zheng YN, Chen C, Li YR, Li W (2019). Arginyl-fructosyl-glucose, a major Maillard reaction product of red ginseng, attenuates cisplatin-induced acute kidney injury by regulating nuclear factor κB and phosphatidylinositol 3-kinase/protein kinase B signaling pathways. *Journal of Agricultural and Food Chemistry* **67**: 5754–5763. DOI 10.1021/acs.jafc.9b00540.

Li Y, Cao Y, Wang F, Li C (2014). Scrotal heat induced the Nrf2-driven antioxidant response during oxidative stress and apoptosis in the mouse testis. *Acta Histochemica* **116**: 883–890. DOI 10.1016/j.acthis.2014.02.008.

Li Z, Li Y, Zhou X, Dai P, Li C (2018). Autophagy involved in the activation of the Nrf2-antioxidant system in testes of heat-exposed mice. *Journal of Thermal Biology* **71**: 142–152. DOI 10.1016/j.jtherbio.2017.11.006.

Lin C, Choi YS, Park SG, Gwon LW, Lee JG, Yon JM, Baek IJ, Lee BJ, Yun YW, Nam SY (2016). Enhanced protective effects of combined treatment with β-carotene and curcumin against hyperthermic spermatogenic disorders in mice. *BioMed Research Internation* **2016**: 1–8. DOI 10.1155/2016/2572073.

Liu XX, Shen XF, Liu FJ (2016). Screening targeted testisspecific genes for molecular assessment of aberrant sperm quality. *Molecular Medicine Reports* **14**: 1594–1600. DOI 10.3892/mmr.2016.5434.

Cargnello M, Roux PP (2011). Activation and function of the MAPKs and their substrates, the MAPK-activated protein kinases. *Microbiology and Molecular Biology Reviews* **75**: 50–83. DOI 10.1128/MMBR.00031-10.

Mi XJ, Hou JG, Jiang S, Liu Z, Tang S, Liu XX, Wang YP, Chen C, Wang Z, Li W (2019). Maltol mitigates thioacetamide-induced liver fibrosis through TGF-beta1-mediated activation of PI3K/Akt signaling pathway. *Journal of Agricultural and Food Chemistry* **67**: 1392–1401. DOI 10.1021/acs.jafc.8b05943.

Niu T, Fu G, Zhou J, Han H, Chen J, Wu W, Chen H (2020). Floridoside exhibits antioxidant properties by activating HO-1 expression via p38/ERK MAPK pathway. *Marine Drugs* **18**: 105. DOI 10.3390/md18020105.

Park HJ, Choe S, Park NC (2016). Effects of Korean red ginseng on semen parameters in male infertility patients: A randomized, placebo-controlled, double-blind clinical study. *Chinese Journal of Integrative Medicine* **22**: 490–495. DOI 10.1007/s11655-015-2139-9.

Park YJ, Cho M, Choi G, Na H, Chung Y (2020). A critical regulation of Th17 cell responses and autoimmune neuro-inflammation by ginsenoside Rg3. *Biomolecules* **10**: 122. DOI 10.3390/biom10010122.

Paul C, Murray AA, Spears N, Saunders PT (2008). A single, mild, transient scrotal heat stress causes DNA damage, subfertility and impairs formation of blastocysts in mice. *Reproduction* **136**: 73–84. DOI 10.1530/REP-08-0036.

Phi LTH, Wijaya YT, Sari IN, Kim KS, Yang YG, Lee MW, Kwon HY (2019). 20(R)-ginsenoside Rg3 influences cancer stem cell properties and the epithelial-mesenchymal transition in colorectal cancer via the SNAIL signaling axis. *Onco Targets and Therapy* **12**: 10885–10895. DOI 10.2147/OTT.S219063.

Phuge SK (2017). High temperatures influence sexual development differentially in male and female tadpoles of the Indian skipper frog, *Euphlyctis cyanophlyctis*. *Journal of Biosciences* **42**: 449–457. DOI 10.1007/s12038-017-9689-2.

Qi LW, Wang CZ, Yuan CS (2011). Ginsenosides from American ginseng: chemical and pharmacological diversity. *Phytochemistry* **72**: 689–699. DOI 10.1016/j.phytochem.2011.02.012.

Qin M, Rao ZR, Wang JJ, Zhao BM, Yang Q, Wang XX, Huang YX (2007). Influence of intrathecal injection of fluorocitrate on the protective effect of electroacupuncture on gastric mucosa in high humid heat stress rats. *Zhen Ci Yan Jiu* **32**: 158–162.

Rao M, Zhao XL, Yang J, Hu SF, Lei H, Xia W, Zhu CH (2015). Effect of transient scrotal hyperthermia on sperm parameters, seminal plasma biochemical markers, and oxidative stress in men. *Asian Journal of Andrology* **17**: 668–675. DOI 10.4103/1008-682X.146967.

Ren S, Leng J, Xu XY, Jiang S, Wang YP, Yan XT, Liu Z, Chen C, Wang Z, Li W (2019). Ginsenoside Rb1, a major saponin from *Panax ginseng*, exerts protective effects against acetaminophen-induced hepatotoxicity in mice. *American Journal of Chinese Medicine* **47**: 1815–1831. DOI 10.1142/S0192415X19500927.

Shen H, Fan X, Zhang Z, Xi H, Ji R, Liu Y, Yue M, Li Q, He J (2019). Effects of elevated ambient temperature and local testicular heating on the expressions of heat shock protein 70 and androgen receptor in boar testes. *Acta Histochemica* **121**: 297–302. DOI 10.1016/j.acthis.2019.01.009.

Shikone T, Billig H, Hsueh AJ (1994). Experimentally induced cryptorchidism increases apoptosis in rat testis. *Biology of Reproduction* **51**: 865–872. DOI 10.1095/biolreprod51.5.865.

Sinha APH, Lue Y, Diaz-Romero M, Yen PH, Wang C, Swerdloff RS (2003). Deciphering the pathways of germ cell apoptosis in the testis. *Journal of Steroid Biochemistry and Molecular Biology* **85**: 175–182. DOI 10.1016/S0960-0760(03)00193-6.

Stahli A, Maheen CU, Strauss FJ, Eick S, Sculean A, Gruber R (2019). Caffeic acid phenethyl ester protects against oxidative stress and dampens inflammation via heme oxygenase 1. *International Journal of Oral Science* **11**: 1418. DOI 10.1038/s41368-018-0039-5.

Stival C, Puga Molina Ldel C, Paudel B, Buffone MG, Visconti PE, Krapf D (2016). Sperm capacitation and acrosome reaction in mammalian sperm. *Advances in Anatomy, Embryology and Cell Biology* **220**: 93–106. DOI 10.1007/978-3-319-30567-7_5.

Sui J, Feng Y, Li H, Cao R, Tian W, Jiang Z (2019). Baicalin protects mouse testis from injury induced by heat stress. *Journal of Thermal Biology* **82**: 63–69. DOI 10.1016/j.jtherbio.2019.03.009.

Sui X, Kong N, Ye L, Han W, Zhou J, Zhang Q, He C, Pan H (2014). p38 and JNK MAPK pathways control the balance of apoptosis and autophagy in response to chemotherapeutic agents. *Cancer Letters* **344**: 174–179. DOI 10.1016/j.canlet.2013.11.019.

Wang RS, Yeh S, Tzeng CR, Chang C (2009). Androgen receptor roles in spermatogenesis and fertility: Lessons from testicular cell-specific androgen receptor knockout mice. *Endocrine Reviews* **30**: 119–132. DOI 10.1210/er.2008-0025.

Xing JJ, Hou JG, Ma ZN, Wang Z, Ren S, Wang YP, Liu WC, Chen C, Li W (2019). Ginsenoside Rb3 provides protective effects against cisplatin-induced nephrotoxicity via regulation of AMPK-/mTOR-mediated autophagy and inhibition of apoptosis *in vitro* and *in vivo*. *Cell Proliferation* **52**: 37. DOI 10.1111/cpr.12627.

Xu H, Li C, Mozziconacci O, Zhu R, Xu Y, Tang Y, Chen R, Huang Y, Holzbeierlein JM, Schoneich C, Huang J, Li B (2019). Xanthine oxidase-mediated oxidative stress promotes cancer cell-specific apoptosis. *Free Radical Biology and Medicine* **139**: 70–79. DOI 10.1016/j.freeradbiomed.2019.05.019.

Xue P, Yao Y, Yang XS, Feng J, Ren GX (2017). Improved antimicrobial effect of ginseng extract by heat transformation. *Journal of Ginseng Research* **41**: 180–187. DOI 10.1016/j.jgr.2016.03.002.

Zhang JJ, Wang JQ, Xu XY, Yang JY, Wang Z, Jiang S, Wang YP, Zhang J, Zhang R, Li W (2020). Red ginseng protects against cisplatin-induced intestinal toxicity by inhibiting apoptosis and autophagy via the PI3K/AKT and MAPK signaling pathways. *Food & Function* **11**: 4236–4248. DOI 10.1039/D0FO00469C.

Zhang M, Jiang M, Bi Y, Zhu H, Zhou Z, Sha J (2012). Autophagy and apoptosis act as partners to induce germ cell death after heat stress in mice. *PLoS One* **7**: e41412. DOI 10.1371/journal.pone.0041412.

Zhou YD, Hou JG, Liu W, Ren S, Wang YP, Zhang R, Chen C, Wang Z, Li W (2018). 20(R)-ginsenoside Rg3, a rare saponin from red ginseng, ameliorates acetaminophen-induced hepatotoxicity by suppressing PI3K/AKT pathway-mediated inflammation and apoptosis. *International Immunopharmacology* **59**: 21–30. DOI 10.1016/j.intimp.2018.03.030.